Control and Management of Railway System Connected to Microgrid Stations

ZINEB CABRANE AND SOO HYOUNG LEE, (Member, IEEE)

Department of Electrical and Control Engineering, Mokpo National University, Muan-gun, Jeollanam-do 58554, South Korea

Corresponding author: Soo Hyoung Lee (slee82@mokpo.ac.kr)

ABSTRACT The recent railway system is a huge microgrid assembling multiplex structure with distributed active loads, sources and storage devices. The active load represents the train. The sources are a microgrid based on renewable energies. The big problem of the most of electrical train is that they can't recover energy recovery during regenerative breaking phases. another problem of the electrical train is the long charging time from the stations. This paper suggests a techno-economic process for the energy storage by using SCs in the train, with the aim to reduce the energy consumptions. The proposed design of railway station use PV and wind sources, and batteries for energy storage system (ESS). For the train, SCs are implemented to the ESS where they are alimented breaking phases and from stations by a pantograph installed in an air power line in each stop. SCs are distinguished by high characteristics power and a wide number of charge/discharge cycles, they provide low particular energy and a fast charging time. An energy management approach is suggested to control the DC bus by voltage and the buck-boost converter by current. The Sizing of PI controller used for the stabilization of the DC bus of train and station is given. The whole system is modeled in MATLAB-Simulink. Simulations for the train and station show the suitability of the suggested powertrain and control strategy.

INDEX TERMS Energy management, railway system control, energy storage system, supercapacitors.

I. INTRODUCTION

A. MOTIVATION

In the last few decades, generally there are growing in energy using and pollutions [1]. The growing number of citizen traveling between cities has implied the continuous development of mass transit systems as buses, taxies, and trains [2]. However, the use of railway transportation systems other conventional means of transport is widely recognized due to the Carrying capacity of a large number of people. The development of rail transportation allows people to travel quickly. Thereby, growing environmental like climate change and CO2 emissions change issues dictate the requisite for ameliorate the performance energy regulation of railway systems [3], [4]. For these raisons, the electrified railway traffic has become a principal development management of current public transportation networks [5], [6].

The associate editor coordinating the review of this manuscript and approving it for publication was Behnam Mohammadi-Ivatloo.

The production of clean energy from renewable sources have become the hot topics of social development [7]. However, railway system integrates different renewable energy sources, like photovoltaics (PV) and wind turbines. To ensure a continuous power supply and to respond to the charge power of train from station to the train, an energy storage system (ESS) is necessary [8], [9]. In order to manage the overload variation in railway power supply structure in the time of heights commuting hours, a wide number of ESS technologies are implemented in the railway system as a constructive means to improve load needs [6], [10]. The on-board storage augmented the weight and space of a vehicle that encourage the underground storage.

SCs represent an appear energy storage devices characterized with a high power density, a long span life and a wide temperature range, has become the best appropriate storage element match with the functioning characteristics of train system [11]–[14]. By comparing SCs to different energy storage devices like batteries and flywheels, SCs present fast
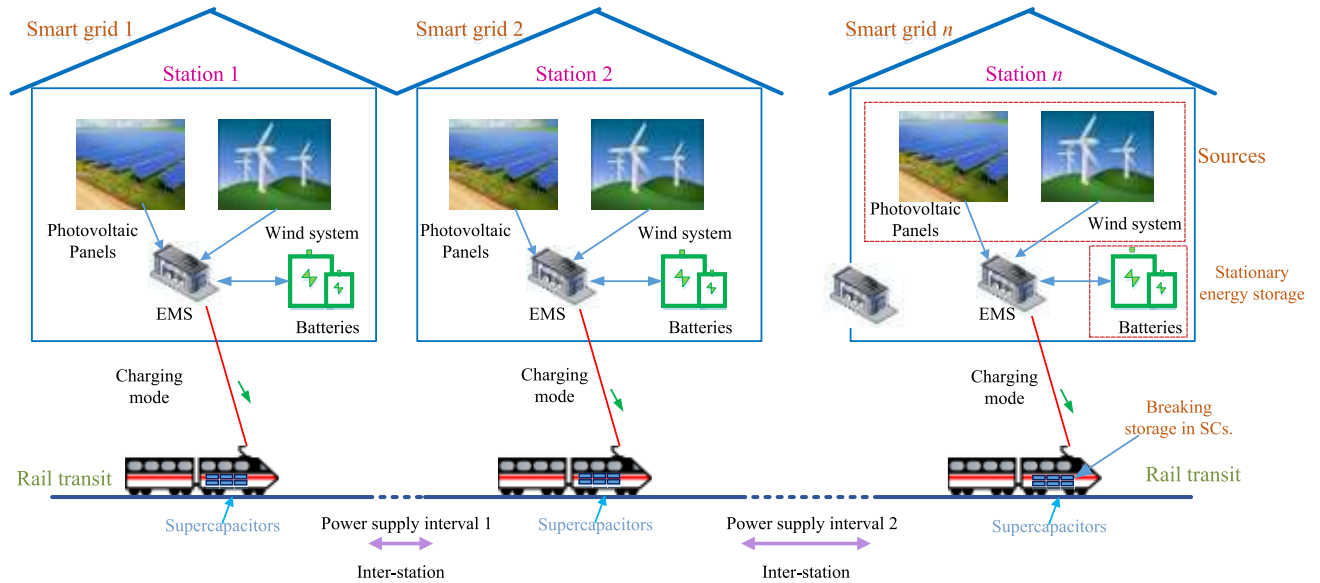
FIGURE 1. Train network traction characteristic.

charging and discharging time because of the high power density, and important potential of energy recovery [15]. In general, ESS with SC is considered like energy buffer accelerating mode of train and recycles the excess of power during the braking mode, realizing a good balance of charge and discharge [16]. SCs are considered a best solution in systems which characterized with different fluctuations. SCs are also used in interruptible power systems to stabilized the power and bus voltage. The energy storage in railway system presents a challenge for researches [17], [18].

Energy management system (EMS) is currently a big challenge in large-scale complex energy distribution networks like railway structure. Most of EMS researches in railway structure interest on ameliorating the railway system technologically. EMS on the system level with an integrated strategy into the railway structure often is ignored [19], [20]. The optimal control theory for railway vehicle is presented in many articles [21], [22]. EMS is implemented to control and connect different devices in railway system, energy storage devices, sources and train.

B. LITERATURE
The railway system has been studied successfully in many articles by researches such as: Jiang presents a fast inspection method for high-speed railway infrastructure monitoring [23], Feng gives the electric railway smart microgrid system with integration of multiple energy systems and power-quality improvement [24]. Khayyam gives railway system energy management optimization demonstrated at offline and online case studies [19], Zhang presents the method using a prediction approach [24], He shown the energy harvesting approach for railway wagon monitoring sensor with high reliability and simple structure [25], Sun presents the hybrid method for life prediction of railway [26], Novak presents the hierarchical model predictive control

for coordinated electric railway traction system energy management [27], Sengor gives the energy management of a smart railway station considering regenerative braking and stochastic behaviour of ESS and PV Generation [28].

C. CONTRIBUTIONS
The proposed system, is composed of two parts: the first one concern the stations, the second one is addressed to the control of trains. The stations are composed PV and wind fields where the energy storage is insured by batteries. The trains are composed by SCs and engine. SCs are used because of their high power. The innovative contributions given in this article are as follows:

- A design of train implementing SCs for energy storage alimented from stations and breaking phases.
- A new EMS is suggested to control the DC bus by voltage and the buck-boost converter by current.
- Sizing of PI controller used for the stabilization of the DC bus of train and station. A design of railway station using PV and wind sources, and batteries for energy storage.

Remainders of paper are as follows: system description is depicted in Section II. The system modelling and management is designed in Section II. The simulation and validation expounded in Section IV. In Finally, Section V draws the conclusion.

II. SYSTEM DESCRIPTION
A. GLOBAL SYSTEM DESCRIPTION
The implementing of the rail transit and energy strategy is illustrated in Fig 1. The railway system is constructor of two systems. The first one is stationary system which represents the different stations. Each station is composed by a main energy sources which are PV panels and wind system. The energy provided from main sources is stored in batteries.
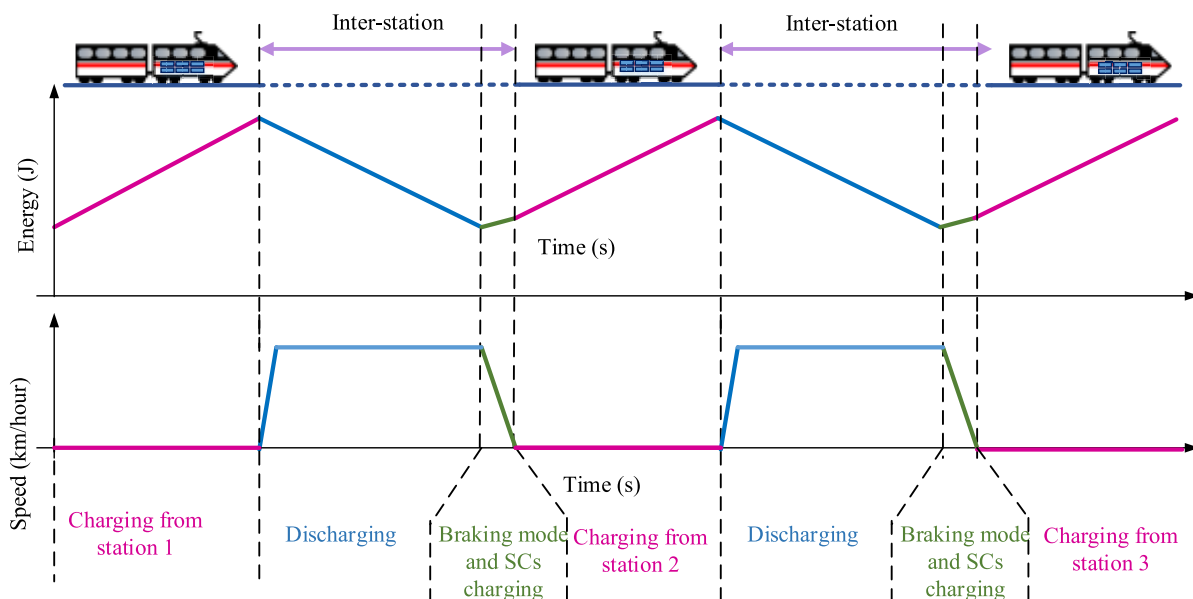
FIGURE 2. Power and speed change between train and stations.

The conversion of energy is insured by boost, buck-boost converters and inverter. Wind system is coupled to the DC bus by an inverter. A boost converter is used to connect PV panels to the DC bus. A buck-boost converter is implemented to couple batteries to the DC bus. The different stations have the same structure and components. The control of the DC bus is insured with an EMS based on PI control. The second one is the mobile system which represents the trains. Each train is composed by motors and supercapacitors. The transfer of energy from SCs to the motors is insured by a buck-boost converter.

B. DISTRIBUTION OF ENERGY BETWEEN DEVICES

The exchange of energy between different devices is given in Fig. 2. The railway system is divided in different stations. The distance between station is more than 10Km. Trains stop in each station between 5 and 15 minutes. During this trains stop, the motors train stop working and SCs charge from batteries installed in the stationary station by a buck-boost converter. The charge of SCs in the stations is insured by the pantograph connected the roof of the trains.

During of the circulation of train between stations, the SCs supply the need of energy. During the braking of the train the energy is returned to SCs. This energy which is produced by different train will be stored locally and produced later in next phases during its acceleration. However, the train in functioning as a load during tracking mode and as a source of the power during braking mode. The stations and trains are connected and mutually communicated.

The different state functioning of rail train engine resolves the form of electrical power exchange. During the traction of the engine, the alternator mode, the train is in the acceleration conditions. In this case, the electric power circle
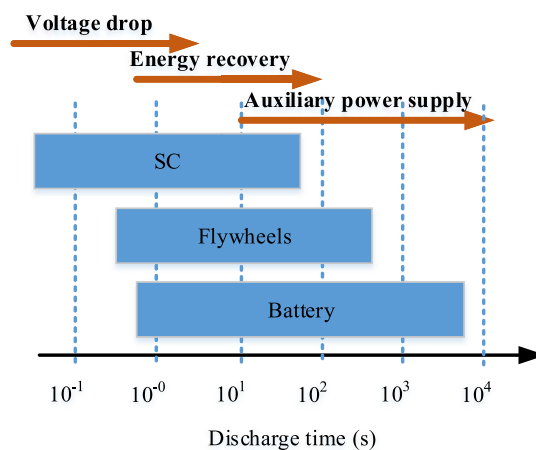

FIGURE 3. Classification of ESS technologies [22].

in the forward direction, that is transformed into kinetic energy from the traction system. during the traction engine, the power generation phase, the train is in braking and deceleration mode. At this moment, the electric energy circle in the inverse direction, and the kinetic energy given by the train during braking is used by the auxiliary installations of the train itself, with most of them being fed back to the SCs and used by the train in the same power supply phase.

The installation of the storage devices reduces the energy line losses, because the power circle though the line is minimized, and the smoother voltage profiles without the request of changing the infrastructure of the structure. The implementation of SCs on a vehicle however need a large space, adding at the same time extra weight that can affect significantly the dynamic specifications of the train.
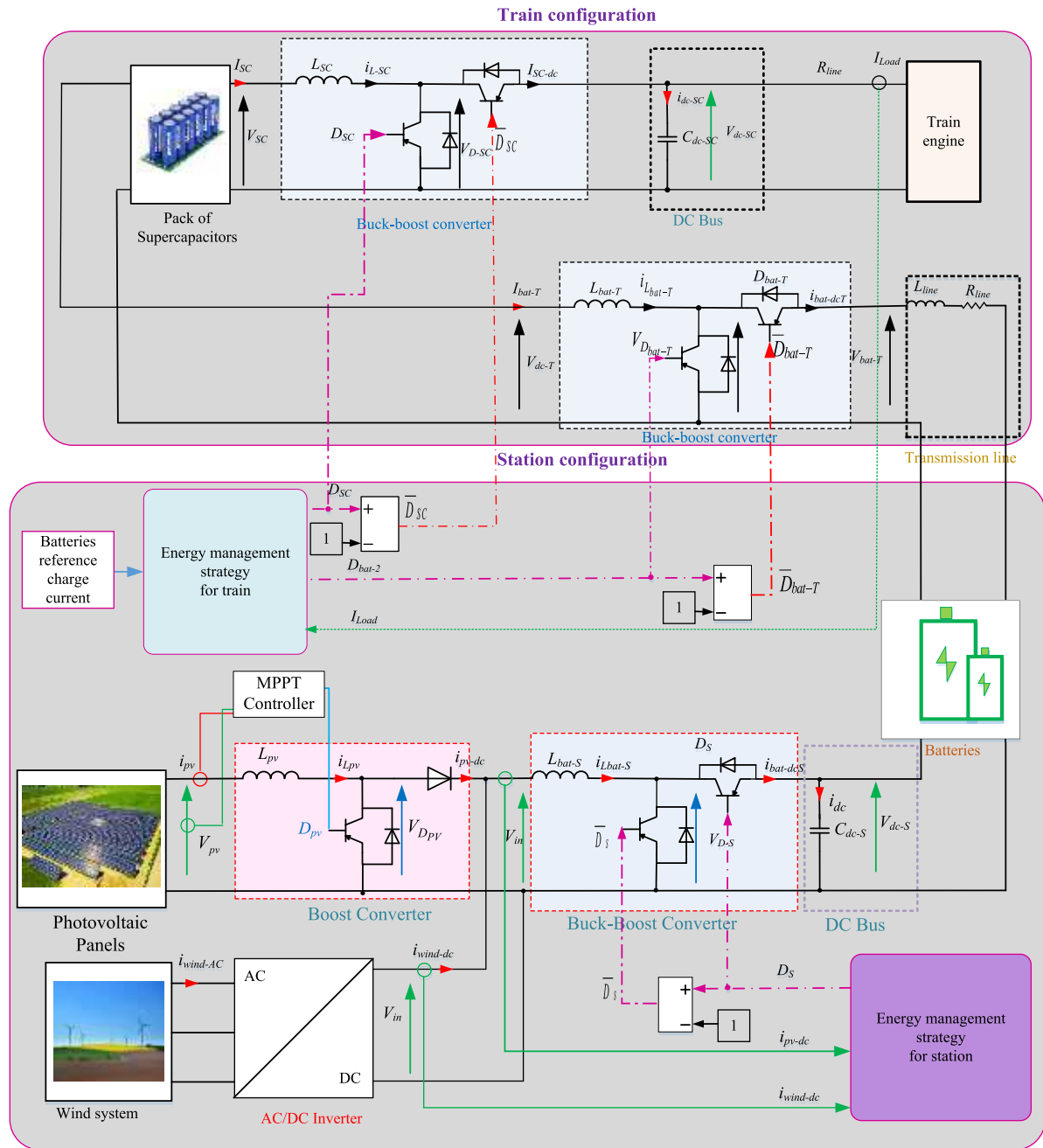
FIGURE 4. Configuration of the train model.

The train power is 3.5MW. The energy delivered by SCs is estimated at approximately 210MJ (corresponding to 3.5MW for 60 s).

C. CHOOSE OF ENERGY STORAGE DEVICES

The most suitable ESS technologies able to meet the railway system is presented in Fig. 3. Flywheels and supercapacitors are performed by high specific power and a large number of charge/discharge cycles. However, they present low specific energy [22]. In fact, they can be implemented in urban rail transit or metro stricture. Batteries represents a low

discharge time. Supercapacitors present the fastest energy storage dispositive in terms of charging and discharging time. For this raison, the use of SCs in the braking and acceleration phases gives good resultants and is the most suitable ESS devices for railway system.

III. SYSTEM MODELLING AND ENERGY MANAGEMENT

The DC bus is controlled according to the diagram given in Fig. 4. The EMS is divided in two parts, the first one is the control of the stationary system and the second in the train.

TABLE 1. Mathematical modelling of PV and wind system.

Device	Mathematical model		Abbreviations
PV [22]	PV current I_{pv}	$I_{pv} = I_{ph} - I_d - I_r$ $$I_s\left(\exp\left(\frac{q\left(V_{pv}+I_{pv}R_s\right)}{n_{s-pv}AkT_c}\right)-1\right)$$ $$\frac{I_{pv}R_s + V_{pv}}{R_p}$$	I_{ph} : Photocurrent I_S : Cell dark saturation current $n_{s\text{-}pv}$: Number of PV cells T_C : Cell's working temperature T_n : Cell's reference temperature
	PV current I_{pv}	$$I_{pv} = I_{ph} - I_s\left(\exp\left(\frac{q\left(V_{pv}+I_{pv}R_s\right)}{n_{s-pv}AkT_c}\right)-1\right)$$ $$-\frac{I_{pv}R_s+V_{pv}}{R_p}$$	A : Ideal factor R_S : Series resistor R_p : Shunt resistor $I_{s,0}$: Cell's short-circuit current at a 25°C E_g : Energy of the band gap I_r : Solar irradiation I_{ph} : Light-generated current
	saturation current I_s	$$I_S = I_{s,0}\left(\frac{T_n}{T}\right)^3 \exp\left[\frac{qE_g}{Ak}\left(\frac{1}{T_n}-\frac{1}{T}\right)\right]$$	I_n : Solar irradiation at T_C temperature q: Electron charge k: Boltzmann's constant
	Photocurrent I_{ph}	$$I_{ph} = \left(I_{ph,n}+K_I\Delta_T\right)\frac{G}{G_n}$$ $$\Delta_T = T - T_n$$	
Wind	power turbine P_m	$$P_m = \frac{1}{2}C_p\left(\lambda,\beta\right)\rho\frac{A}{2}V_{wind}^3$$	β : blade pitch angle C_p : performance coefficient λ : tip speed ratio of the rotor blade
	$C_p(\lambda; \beta)$	$$C_p = \frac{1}{2}\left(\frac{116}{4}-0.4\beta-0.5\right)e^{-\left(\frac{21}{\lambda}\right)}$$	A : turbine swept area λi is a coefficient that is given by the following equation ρ : density of air.
	λi coefficient	$$\frac{1}{\lambda_i} = \frac{116}{\lambda+0.08\beta}-\frac{0.035}{\beta^3+1}$$	
	wind turbine torque T_m	$$T_m = \frac{1}{2}\rho\pi R^3\frac{C_p\left(\lambda\right)}{\lambda}v^2$$ $$= \frac{1}{2}\rho A C_p\left(\lambda\right)v^3\frac{1}{\omega_m}$$	

For the stationary system, the wind system produces a AC power. It is coupled to the DC bus by using a AC-DC inverter. The PV system is implemented to the same bus by using a Boost converter. An MPPT maximum power point tracking system is implemented to stabilized the PV power and voltage. A Buck-Boost converter is applied to stabilized the DC bus voltage V_{d-S} and to charge the batteries. A line transmission is presented by a resistance and inductance.

For the train system, a Buck-Boost converter is implemented to couple batteries to SCs. Another Buck-Boost is implemented to couple SCs train engine and to stabilize the voltage to 2KW. A capacitor is implemented in parallel to the engine and the buck-boost converter in order to filter the power fluctuation from the converters. The EMS gives the control of the converters. The mathematical modelling of PV and wind system are given in Table 1. The mathematical modelling of SCs and batteries are given in Table 2. The chosen SCs model two branches model. The using batteries model is CIMAT batteries.

The buck-Boost converter is reversible in current. The modelling of this converter is given in Fig. 5 [8].

In the active phase, the switch is closed, the input voltage is given by:

$$v_{L-SC} = V_{sc} = L_{sc}\frac{di_{L-SC}}{dt} \tag{1}$$

$$\frac{di_{L-SC}}{dt} = \frac{V_{sc}}{L_{sc}} \tag{2}$$

where L_{SC} is the inductance, V_{SC} is the SCs voltage, C_{dc-SC} is the SCs buck-boost capacitor.

In the Freewheeling phase, the switch is open and the inductor current cannot fluctuate instantaneously. The input voltage is defined by the following equations:

$$v_{L-SC} = V_{SC} - V_{dc} = L_{SC}\frac{di_{L-SC}}{dt} \tag{3}$$

$$\frac{di_{L-SC}}{dt} = \frac{V_{SC} - V_{dc}}{L_{SC}} \tag{4}$$

TABLE 2. Mathematical modelling of scs and battery system.

| Device	Mathematical model		Abbreviations
SC [23]	SC voltage	$U_{SC} = N_{S-SC} v_{SC} = N_{S-SC} v_1 + R_1 \dfrac{I_{SC}}{N_{P-SC}}$	C_0: capacity (in F) C_v: constant parameter
	SC capacity	$C_1 = C_0 + C_v . v_1.$	
	v_2 voltage	$v_2 = \dfrac{1}{C_2} \int i_2 dt = \dfrac{1}{C_2} \int \dfrac{1}{R_2}(v_1 - v_2)dt.$	Q_1: charge $R_1 C_1$ presents the immediate behavior of SCs during fast charge/discharge
	current i_1	$i_1 = C_1 . \dfrac{dv_1}{dt} = \dfrac{dQ_1}{dt} = (C_0 + C_v . v_1) \dfrac{dv_1}{dt}$	$R_2 C_2$ presents the internal energy distribution at the final of charge/ discharge
	charge Q_1	$Q_1 = C_0 . v_1 + \dfrac{1}{2} C_v . v_1^2$	
Battery [7]	Battery voltage	$V_{bat} = n_b . E_b + n_b . R_i . I_{bat}$	R_i: internal resistance of battery V_{bat}: battery voltage
	expression between I_{10} and C_{10} current	$\dfrac{C_{bat}}{C_{10}} = \dfrac{1.65}{1 + 0.65 . \left(\dfrac{I_{bat}}{I_{10}}\right)^{0.9}}(1 + 0.005.\Delta T)$	I_{bat}: battery current n_b: cells in series E_b: electromotive force as a function of the battery state of charge (denoted SoC) C_{bat}: capacity of battery yields the quantity of energy
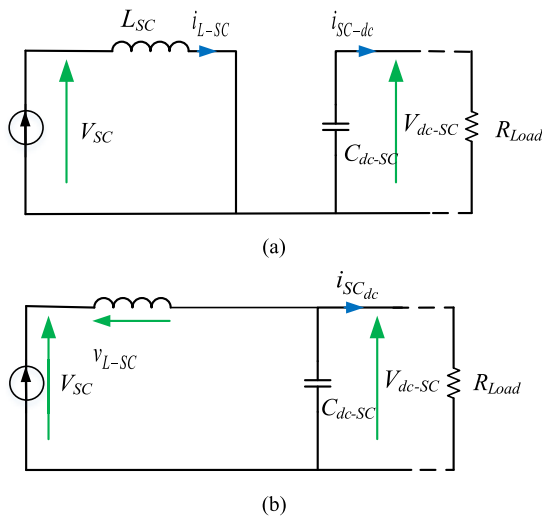
FIGURE 5. Electrical schema of a buck-boost converter. (a) Active phase, (b) Freewheeling phase.

The main equation of the buck-boost converter is given by

$$L_{SC} \frac{di_{L-SC}}{dt} = V_{SC} - (1 - D_{SC})V_{dc} \qquad (5)$$

IV. CONTROL OF THE DC BUS VOLTAGE OF DIFFERENT SYSTEMS OF TRAIN AND STATION

The principle of the control system of SC, train and stationary system are described in Fig. 6. The PI controllers F(s), H(s) and J(s) calculate the reference current of the DC bus of SC system, the train system and the stationary system, $i_{SC-dc-ref}$, $i_{bat-dcT-ref}$ and $i_{bat-dcS-ref}$, respectively. The PI controllers G(s), I(s) and K(s) calculate the duty cycle of SC system D_{SC}, train system D_T and the stationary system D_S, respectively.

The management of the three DC bus is insured with a voltage control. The calculating of the parameters of this PI controller (F(s), H(s) and J(s)) is given by the following equations:

$$C_{dc-SC} \frac{dV_{dc-SC}}{dt} = i_{L-SC}(1 - D_{SC}) - \frac{V_{dc-SC}}{r_{L-SC}} - i_{SC-dc} \qquad (6)$$

$$L_{SC} \frac{di_{L-SC}}{dt} = V_{SC} - (1 - D_{SC})V_{dc-SC} \qquad (7)$$

where $\beta_{SC} = 1 - D_{SC}$. Then,

$$C_{dc-SC} \frac{dV_{dc-SC}}{dt} = i_{L-SC}\beta_{SC} - \frac{V_{dc-SC}}{r_{L-SC}} - i_{SC-dc} \qquad (8)$$

$$L_{SC} \frac{di_{L-SC}}{dt} = V_{SC} - \beta_{SC} V_{dc-SC} \qquad (9)$$

Thereby, the dynamic equation is expressed as:

$$C_{dc-SC} \frac{dV_{dc-SC}}{dt} = i_{L-SC} \frac{V_{SC}}{V_{dc-SC}} - \frac{V_{dc-SC}}{r_{L-SC}} - i_{SC-dc} \qquad (10)$$

By supposing $X = V_{dc-SC}^2$ is replaced, the linear function is expressed by:

$$\frac{dX}{dt} = 2V_{dc-SC} \frac{dV_{dc-SC}}{dt} \qquad (11)$$

where

$$\frac{dV_{dc-SC}}{dt} = \frac{1}{2V_{dc-SC}} \frac{dX}{dt} \qquad (12)$$

The main equation is given:

$$C_{dc-SC} \frac{dX}{dt} = 2i_{L-SC}V_{SC} - 2\frac{X}{r_{L-SC}} - 2i_{SC-dc}V_{dc-SC} \qquad (13)$$
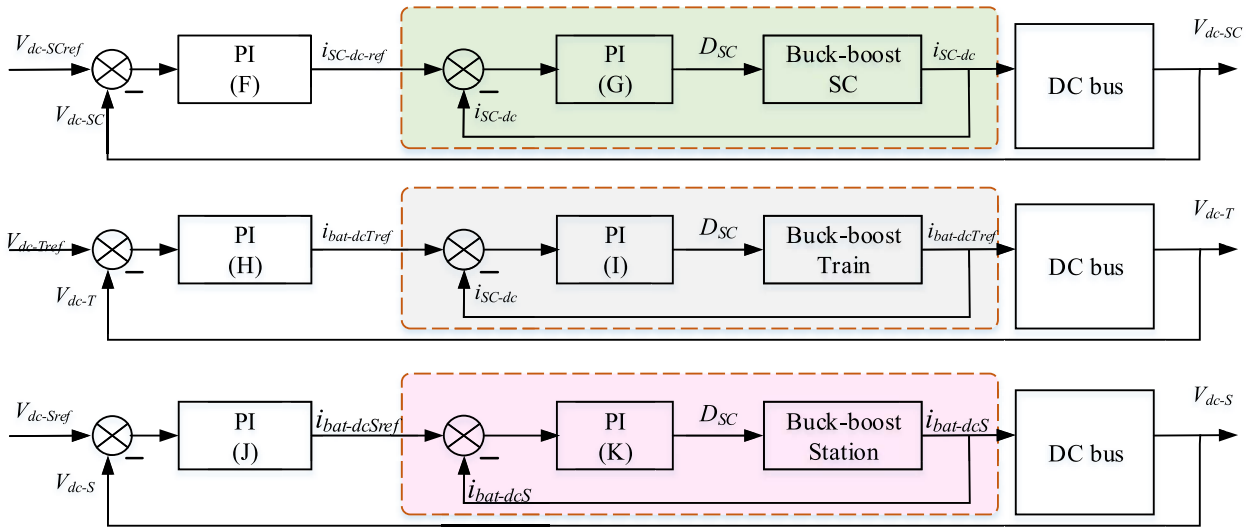
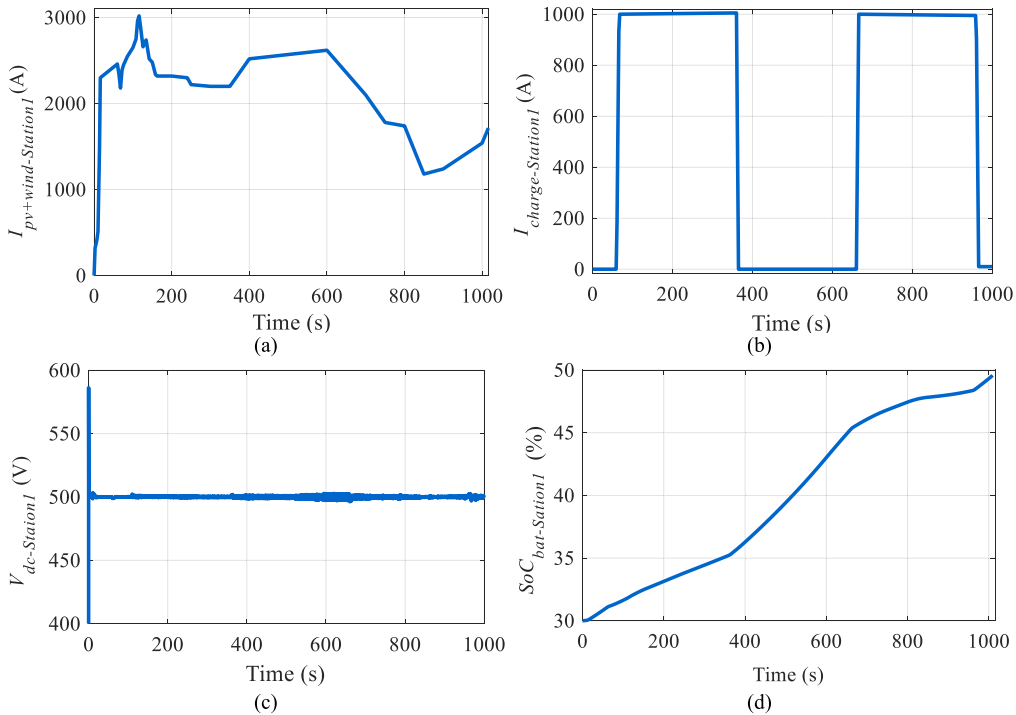**FIGURE 6.** Bloc diagram of the energy management.

FIGURE 7. Simulation test of station 1. (a) PV and wind current of station 1. (b) Charge current from station 1. (c) DC bus voltage of station 1. (d) SoC of batteries of station 1.

The TF (transfer function) of between voltage and current in Laplace domain is given by

$$FTx(s) == \frac{V_{dc-SC(s)}}{I_{SC-dc}(s)} = \frac{V_{SC}\, r_{L-SC}}{\frac{r_{L-SC}C_{dc-SC}}{2}s + 1} \quad (14)$$

The TF of the SC system is represented by

$$F(s) = K_{p-SC1} + \frac{K_{i-SC1}}{s} \quad (15)$$

where K_{i-SC1} and K_{p-SC1} are the integral and proportional gain used for SCs system control, respectively.

The TF of the train system is represented by

$$H(s) = K_{p-T1} + \frac{K_{i-T1}}{s} \quad (16)$$

K_{i-T1} and K_{p-T1} are the integral and proportional used for the train system control, respectively. The transfer function of the stationary system is expressed by the following equation.

$$J(s) = K_{p-S1} + \frac{K_{i-S1}}{s} \quad (17)$$

K_{i-S1} and K_{p-S1} are the integral and proportional gain used for the stationary system control, respectively. From
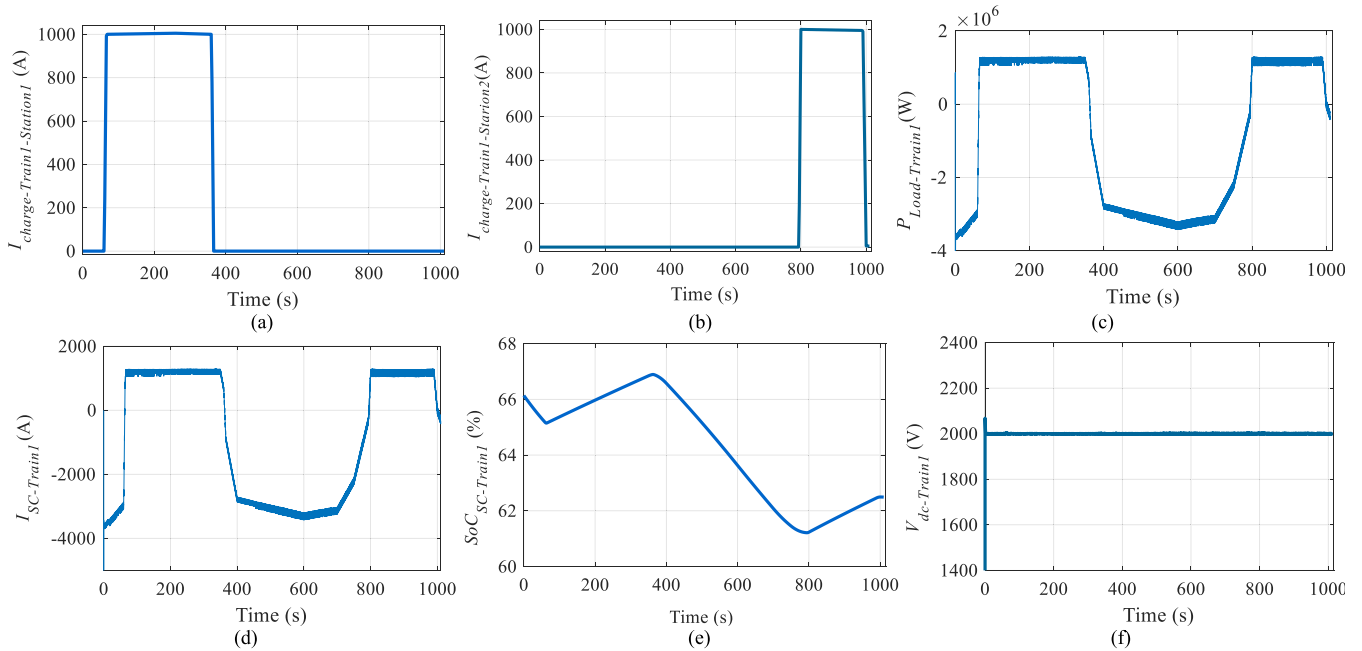
FIGURE 8. Simulation test of train 1. (a) Charge current of train 1 from station 1. (b) Charge current of train 1 from station 2. (c) Load power of train 1. (d) SCs current of train 1. (e) SoC of SCs of train 1. (f) DC bus voltage of train 1.

equation (14) and (15) we deduce the following expression:

$FTBF(s)$

$$= \frac{K_{p-SC1}r_{L-SC}V_{SC}\left(s + \frac{K_{i-SC1}}{K_{p-SC1}}\right)}{K_{p-SC1}r_{L-SC}V_{SC}\left(s + \frac{K_{i-SC1}}{K_{p-SC1}}\right) + s\left(\frac{r_{L-SC}C_{dc-SC}}{2}s + 1\right)} \quad (18)$$

which gives (19), as shown at the bottom of the next page.

The closed-loop transfer function is the SC system is given by (20), as shown at the bottom of the next page.

By identifying the denominator with that of the canonical form the SC system, we deduce

$$\begin{cases} \omega_n^2 = \frac{2}{C_{SC}}V_{SC}K_{iSC1} \\ \\ K_{i-SC1} = \frac{\omega_{n-SC}^2 C_{dc-SC}}{2V_{SC}} \end{cases} \quad (21)$$

where

$$\begin{cases} 2\xi_{SC}\omega_{n-SC} = \frac{2}{r_{L-SC}C_{dc-SC}}\left(K_{p-SC1}r_{L-SC}V_{SC} + 1\right) \\ \\ K_{p-SC1} = \frac{\xi_{SC}\omega_{n-SC}r_{L-SC}C_{dc-SC} - 1}{r_{L-SC}V_{SC}} \end{cases} \quad (22)$$

where $\square_{n-SC}$ is the pulsation for SC system, ξ_{SC} is the damping coefficient for SC system.

K_{i-T1} and K_{p-T1} are the integral and proportional used for the train system control, respectively. They are expressed by:

$$K_{i-T1} = \frac{\omega_{n-T}^2 C_{dc-T}}{2V_{dc-T}} \quad (23)$$

$$K_{p-T1} = \frac{\xi_T\omega_{n-T}r_{L-T}C_{dc-T} - 1}{r_{L-T}V_{dc-T}} \quad (24)$$

where $\square_{n-SC}$ is the pulsation used for train system, ξ_{SC} is the damping coefficient used for train system.

K_{i-S1} and K_{p-S1} are the integral and proportional gain used for the stationary system control, respectively. They are expressed by:

$$K_{i-S1} = \frac{\omega_{n-S}^2 C_{dc-S}}{2V_{dc}} \quad (25)$$

$$K_{p-S1} = \frac{\xi_S\omega_{n-S}r_{L-S}C_{dc-S} - 1}{r_{L-S}V_{dc}} \quad (26)$$

where $\square_{n-SC}$ is the pulsation used for stationary system, ξ_{SC} is the damping coefficient used for stationary system.

The control of the buck-boost converter is insured by a current control. The calculating of the parameters of this PI controller (G(s), I(s) and K(s)) is given by the same methodology and is represented by the following equations:

$$V_{SC} = L_{SC}i_{L-SC}(s)s + R_{Load}i_{L-SC}(s) \\ + (1 - D_{SC}(s))V_{dc-SC} \quad (27)$$

The D_{SC} and I_{SC} is expressed as follows:

$$\frac{I_{SC}(s)}{D_{SC}(s)} = \frac{\frac{V_{dc-SC}}{R_{Load}}}{1 + \frac{L_{SC}}{R_{Load}}s} \quad (28)$$

The TF of the SC system is given by the following equation.

$$G(s) = \frac{K_{i-SC2}\left(1 + \frac{K_{p-SC2}}{K_{i-SC2}}s\right)}{s} \quad (29)$$

The TF of the stationary system is expressed by the following equation.

$$I(s) = \frac{K_{i-T2}\left(1 + \frac{K_{p-T2}}{K_{i-T2}}s\right)}{s} \quad (30)$$

The TF of the stationary system is expressed by the following equation.

$$K(s) = \frac{K_{i-S2}\left(1 + \frac{K_{p-S2}}{K_{i-S2}}s\right)}{s} \quad (31)$$

In order to simplify the transfer function of the system, a pole/zero and imposing compensation are assumed: $\frac{K_{p-SC2}}{K_{i-SC2}} = \frac{L_{SC}}{R_{Load}}$. The new CLTF(s) becomes

$$CLTF(s) = \frac{1}{1 + \frac{R_{Load}}{V_{dc-SC}K_{i-SC2}}s} \quad (32)$$

where

$$\tau_{SC} = \frac{R_{Load}}{V_{dc-SC}K_{i-SC2}} \quad (33)$$

Then, K_{i-SC2} and K_{p-SC2} are the integral and proportional used for the SC system control, respectively. They are expressed by:

$$K_{i-SC2} = \frac{R_{Load}}{\tau_{SC}V_{dc-SC}} \quad (34)$$

$$K_{p-SC2} = \frac{L_{SC}}{\tau_{SC}V_{dc-SC}} \quad (35)$$

K_{i-T2} and K_{p-T2} used for the train system control is expressed by:

$$K_{i-T2} = \frac{R_{Load-SC}}{\tau_T V_{dc-T}} \quad (36)$$

$$K_{p-T2} = \frac{L_{bat-T}}{\tau_T V_{dc-T}} \quad (37)$$

K_{i-S2} and K_{p-S2} are the integral and proportional used for the train system control, respectively. They are expressed by:

$$K_{i-S2} = \frac{R_{Load-bat}}{\tau_S V_{dc-S}} \quad (38)$$

$$K_{p-S2} = \frac{L_{bat-S}}{\tau_S V_{dc-S}} \quad (39)$$

τ_{SC}, τ_S and τ_T are the time constant used for SCs, train and stationary system, respectively.

V. SIMULATION RESULTS

For test the feasibility of the presented strategy, a model of the whole system is built by Matlab/Simulink software. The proposed simulation test is presented by one station (station 1) and two trains (train 1 and train2). The simulation tests are proposed with the same parameters of trains and stations during 1000s. The scenario of wind, solar irradiation and temperature is proposed variable.

The initial state of charge of batteries used in station 1 is $SoC_{bat-Station1} = 30\%$.

The initial state of charge of SCs used in train 1 is $SoC_{SC-Train1} = 66\%$.

The initial state of charge of SCs used in train 2 is $SoC_{SC-Train2} = 66\%$.

Fig. 7 represents the simulation test of station 1. This station is proposed by a microgrid using PV and wind as a sources. The energy storage is insured by batteries. Fig. 8 and 9 represent the simulation tests of train 1 and train 2, respectively. In this simulation test, train 1 and train 2 charge from station 1 in different duration. Train 1 reach station 1 at t=50s and train 2 reach station 1 at t=650s. Fig. 7(a) represents the PV and wind current that is varied between 1200A and 3000A.

The charge current of station 1 is illustrated in Fig. 7(b). Train 1 charge from station 1 between t=50s and t=350s with a constant current of $I_{charge-Station1} = 1000A$ for a duration of five minutes. Train 2 charge from station 1 between t=650s and t=950s with a constant current of $I_{charge-Station1} = 1000A$ for a duration of five minutes. The DC bus voltage of station 1 in given in Fig. 7(c). It is fixed at 500V. The stat of charge of batteries of station 1 is given in Fig. 7(d). It is represented between 30% and 50%. Train 1 charge from station 1 between t=50s and t=350s, and charge from station 2 between t=800s and t=1000s. The charge current of SCs from station 1 and 2 used for train 1 is given in Fig. 8(a and b), respectively. Power and current of SCs are shown in Fig. 8(c and d), respectively. The power and current are positive and constant in the charging mode and negative in the traction mode. The DC bus voltage of train 1 is 2000V and is given in Fig. 8(e). The stat of charge of SCs of train 1 is given in Fig. 8(f). It varies between 61% and 67% that represents an augmentation during charging mode and reduction during traction mode.

Train 2 charge from station 1 between t=650s and t=950s. The charge current of SCs from station 2 used for train 2

$$FTBF(s) = \frac{K_{p-SC1}r_{L-SC}V_{SC}\left(s + \frac{K_{i-SC1}}{K_{p-SC1}}\right)}{\frac{r_{L-SC}C_{dc-SC}}{2}s^2 + \left(K_{p-SC1}r_{L-SC}V_{SC} + 1\right)s + K_{p-SC1}r_{L-SC}V_{SC}\frac{K_{i-SC1}}{K_{p-SC1}}} \quad (19)$$

$$CLTF(s) = \frac{\frac{2}{C_{dc-SC}}K_{p-SC}V_{SC}\left(s + \frac{K_{i-SC1}}{K_{p-SC1}}\right)}{s^2 + \frac{2}{r_{L-SC}C_{dc-SC}}\left(K_{p-SC1}r_{L-SC}V_{SC} + 1\right)s + \frac{2}{C_{dc-SC}}V_{SC}K_{i-SC1}} \quad (20)$$
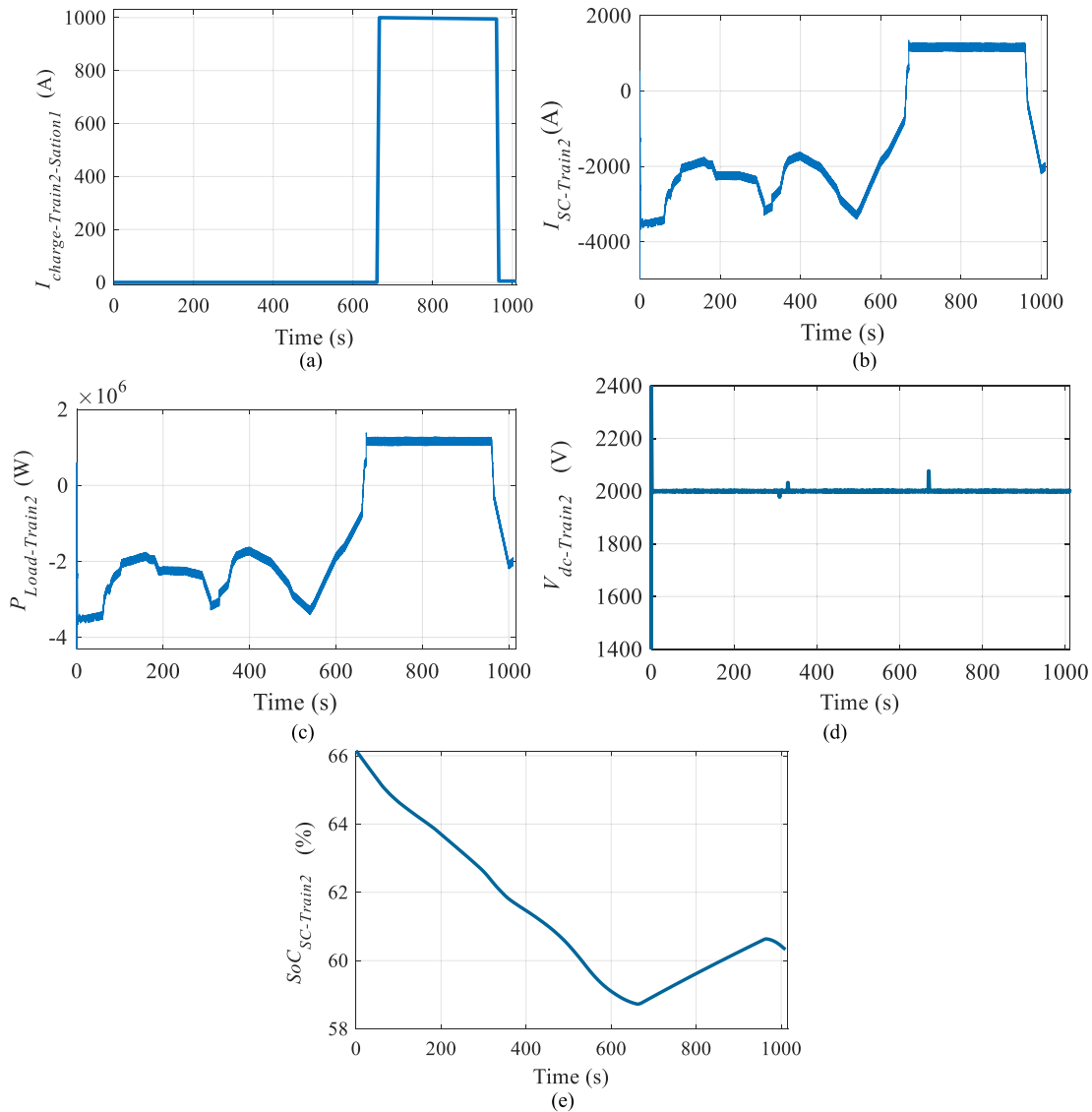
FIGURE 9. Simulation test of train 2. (a) Charge current of train 1 from station 1. (b) SCs current of train 2. (c) Load power of train 2. (d) DC bus voltage of train 2. (e) SoC of SCs of train 2.

is given in Fig. 9(a). The power and SCs current are represented in Fig. 9(b and c), respectively. The DC bus current of train 1 is 2000V and is given in Fig. 9(d). The stat of charge of SCs of train 1 is given in Fig. 9(e). It varies between 69% and 66% that represents an augmentation during charging mode and reduction during traction mode.

The simulation results proof that the proposed energy management system and control system give good results.

VI. CONCLUSION
The proposes techno-economic method for the energy storage by using SCs in the train was presented in this paper. The studied system is devised on two parts: station and train. The design of railway station is presented by using PV and wind as principal sources, and batteries for ESS. The train

is composed by engine and SCs. SCs are implemented to the ESS of the train, where they are alimented from the breaking phases and the stations by a pantograph installed in an air power line in each stop. SCs are used for their fast charge and discharge. An EMS is given in order to stabilized the DC bus. The calculation of parameters of the buck-boost converter are given. The Sizing of the integral and proportional gain controller used for the stabilization of the DC bus of train and station is given. A simulation test was proposed with one station and two trains. The trains recharge from the station in different times. The obtained results showed that the given EMS and system design give good results in order to stabilized the DC bus voltage and reply to the need of energy by the engine. The future work will be reserved to the application of this system with AC engine.

REFERENCES

[1] G. Cui, L. Luo, C. Liang, S. Hu, Y. Li, Y. Cao, B. Xie, J. Xu, Z. Zhang, Y. Liu, and T. Wang, "Supercapacitor integrated railway static power conditioner for regenerative braking energy recycling and power quality improvement of high-speed railway system," *IEEE Trans. Transport. Electrific.*, vol. 5, no. 3, pp. 702–714, Sep. 2019.

[2] F. Ciccarelli, A. Del Pizzo, and D. Iannuzzi, "Improvement of energy efficiency in light railway vehicles based on power management control of wayside lithium-ion capacitor storage," *IEEE Trans. Power Electron.*, vol. 29, no. 1, pp. 275–286, Jan. 2014.

[3] V. A. Kleftakis and N. D. Hatziargyriou, "Optimal control of reversible substations and wayside storage devices for voltage stabilization and energy savings in metro railway networks," *IEEE Trans. Transport. Electrific.*, vol. 5, no. 2, pp. 515–523, Jun. 2019.

[4] T. Ratniyomchai, S. Hillmansen, and P. Tricoli, "Recent developments and applications of energy storage devices in electrified railways," *IET Elect. Syst. Transp.*, vol. 4, no. 1, pp. 9–20, Mar. 2014.

[5] H. Yang, W. Shen, Q. Yu, J. Liu, Y. Jiang, E. Ackom, and Z. Y. Dong, "Coordinated demand response of rail transit load and energy storage system considering driving comfort," *CSEE J. Power Energy Syst.*, vol. 6, no. 4, pp: 749-759, Dec. 2020.

[6] H. Yang, J. Zhang, J. Qiu, S. Zhang, M. Lai, and Z. Y. Dong, "A practical pricing approach to smart grid demand response based on load classification," *IEEE Trans. Smart Grid*, vol. 9, no. 1, pp. 179–190, Jan. 2018.

[7] Z. Cabrane, M. Ouassaid, and M. Maaroufi, "Analysis and evaluation of battery-supercapacitor hybrid energy storage system for photovoltaic installation," *Int. J. Hydrogen Energy*, vol. 41, no. 45, pp. 20897–20907, Dec. 2016.

[8] Z. Cabrane, J. Kim, K. Yoo, and M. Ouassaid, "HESS-based photovoltaic/batteries/supercapacitors: Energy management strategy and DC bus voltage stabilization," *Sol. Energy*, vol. 216, pp. 551–563, Mar. 2021.

[9] Q. Z. Li, X. J. Wang, X. H. Huang, Y. Zhao, Y. W. Liu, and S. F. Zhao, "Research on flywheel energy storage technology for electrified railway," *Proc. CSEE*, vol. 39, no. 7, pp. 2025–2033, Apr. 2019.

[10] H. Yang, Q. Yu, J. Liu, Y. Jia, G. Yang, E. Ackom, and Z. Y. Dong, "Optimal wind-solar capacity allocation with coordination of dynamic regulation of hydropower and energy intensive controllable load," *IEEE Access*, vol. 8, pp. 110129–110139, 2020.

[11] M. Andriollo, R. Benato, M. Bressan, S. Sessa, F. Palone, and R. Polito, "Review of power conversion and conditioning systems for stationary electrochemical storage," *Energies*, vol. 8, no. 2, pp. 960–975, Jan. 2015, doi: 10.3390/en8020960.

[12] K. C. Divya and J. Østergaard, "Battery energy storage technology for power systems—An overview," *Electr. Power Syst. Res.*, vol. 79, no. 4, pp. 511–520, Apr. 2009.

[13] I. Hadjipaschalis, A. Poullikkas, and V. Efthimiou, "Overview of current and future energy storage technologies for electric power applications," *Renew. Sustain. Energy Rev.*, vol. 13, nos. 6–7, pp. 1513–1522, 2009.

[14] Z. Cabrane and S. H. Lee, "Electrical and mathematical modeling of supercapacitors: Comparison," *Energies*, vol. 15, no. 3, p. 693, Jan. 2022.

[15] Z. Cabrane, M. Ouassaid, and M. Maaroufi, "Battery and supercapacitor for photovoltaic energy storage: A fuzzy logic management," *IET Renew. Power Gener.*, vol. 11, no. 8, pp. 1157–1165, 2017.

[16] Z. Yang, F. Zhu, and F. Lin, "Deep-reinforcement-learning-based energy management strategy for supercapacitor energy storage systems in urban rail transit," *IEEE Trans. Intell. Transp. Syst.*, vol. 22, no. 2, pp. 1150–1160, Feb. 2021.

[17] D. Roch-Dupré, T. Gonsalves, A. P. Cucala, R. R. Pecharromán, Á. J. López-López, and A. Fernández-Cardador, "Multi-stage optimization of the installation of energy storage systems in railway electrical infrastructures with nature-inspired optimization algorithms," *Eng. Appl. Artif. Intell.*, vol. 104, Sep. 2021, Art. no. 104370.

[18] H. Lee, S. Jung, Y. Cho, D. Yoon, and G. Jang, "Peak power reduction and energy efficiency improvement with the superconducting flywheel energy storage in electric railway system," *Phys. C, Supercond. Appl.*, vol. 494, pp. 246–249, Nov. 2013.

[19] S. Khayyam, N. Berr, L. Razik, M. Fleck, F. Ponci, and A. Monti, "Railway system energy management optimization demonstrated at offline and online case studies," *IEEE Trans. Intell. Transp. Syst.*, vol. 19, no. 11, pp. 3570–3583, Nov. 2018.

[20] Z. Cabrane, J. Kim, K. Yoo, and S. H. Lee, "Fuzzy logic supervisor-based novel energy management strategy reflecting different virtual power plants," *Electr. Power Syst. Res.*, vol. 205, Apr. 2022, Art. no. 107731.

[21] H. Peng, J. Li, L. Lowenstein, and K. Hameyer, "strategy based on optimal control theory for a fuel cell hybrid railway vehicle," *Appl. Energy*, vol. 267, Jun. 2020, Art. no. 114987.

[22] X. Jiang and S. Wang, "Railway panorama: A fast inspection method for high-speed railway infrastructure monitoring," *IEEE Access*, vol. 9, pp. 150889–150902, 2021.

[23] C. Feng, Z. Gao, Y. Sun, and P. Chen, "Electric railway smart microgrid system with integration of multiple energy systems and power-quality improvement," *Electr. Power Syst. Res.*, vol. 199, Oct. 2021, Art. no. 107459.

[24] Q. Zhang, Z. Yuan, L. Yan, T. Zhang, Y. Miao, and S. Ding, "A railway train number tracking method using a prediction approach," *IEEE Access*, vol. 7, pp. 138288–138298, 2019.

[25] W. He, W. Shi, J. Le, H. Li, and R. Ma, "Geophone-based energy harvesting approach for railway wagon monitoring sensor with high reliability and simple structure," *IEEE Access*, vol. 8, pp. 35882–35891, 2020.

[26] Y. Sun, Y. Cao, M. Zhou, T. Wen, P. Li, and C. Roberts, "A hybrid method for life prediction of railway relays based on multi-layer decomposition and RBFNN," *IEEE Access*, vol. 7, pp. 44761–44770, 2019.

[27] H. Novak, V. Lešić, and M. Vašak, "Hierarchical model predictive control for coordinated electric railway traction system energy management," *IEEE Trans. Intell. Transp. Syst.*, vol. 20, no. 7, pp. 2715–2727, Jul. 2019.

[28] G. Graber, V. Calderaro, V. Galdi, A. Piccolo, R. Lamedica, and A. Ruvio, "Techno-economic sizing of auxiliary-battery-based substations in DC railway systems," *IEEE Trans. Transport. Electrific.*, vol. 4, no. 2, pp. 616–625, Jun. 2018.

[29] D. Rekioua, S. Bensmail, and N. Bettar, "Development of hybrid photovoltaic-fuel cell system for stand-alone application," *Int. J. Hydrogen*, vol. 39, pp. 1604–1611, Jan. 2014.

[30] A. Lahyani, P. Venet, A. Guermazi, and A. Troudi, "Battery/supercapacitors combination in uninterruptible power supply (UPS)," *IEEE Trans. Power Electron.*, vol. 28, no. 4, pp. 1509–1522, Apr. 2013.

ZINEB CABRANE received the B.S. and master's degrees in electrical engineering from the Faculty of Sciences and Techniques, Settat, Morocco, in 2010 and 2012, respectively, and the Ph.D. degree in electrical engineering from the Mohammadia School of Engineers, Mohammed V University, Rabat, Morocco, in 2018. She is currently pursuing the Ph.D. degree in power electronics with Mokpo National University, South Korea. She worked as a Postdoctoral Researcher with the Energy Storage Conversion Laboratory (ESCL), Department of Electrical Engineering, Chungnam National University, Daejeon, South Korea. She is also working as a Postdoctoral Researcher with the Energy Valley Industry-Academic Convergence Center, Naju, South Korea. Her research interests include power electronics, hybrid energy storage systems (HESS), power management systems (PMS), solar vehicle, and microgrid.

SOO HYOUNG LEE (Member, IEEE) received the B.S. and Ph.D. degrees in electrical engineering from the School of Electrical and Electronic Engineering, Yonsei University, Seoul, South Korea, in 2008 and 2012, respectively. From 2012 to 2014, he was a Postdoctoral Research Associate with the School of Electrical and Computer Engineering, Georgia Institute of Technology, Atlanta, GA, USA. From 2014 to 2018, he was a Senior Researcher with the Advanced Power Grid Research Division, Korea Electrotechnology Research Institute, Uiwang, South Korea. He is currently an Assistant Professor with the Department of Electrical and Control Engineering, Mokpo National University, Mokpo, South Korea. His research interests include converter-based microgrid, optimal coordination of distributed generation systems, converter control for distributed generation systems, implementation of multi-level converters for low-voltage ac systems, and non-isolated dc–dc converters for high voltage applications.

● ● ●